ChemPubSoc Europe
DOI: 10.1002/open.201700133
Open Access ChemistryOPEN Reviews

Fluorescence Sensing with Cellulose-Based Materials

Meng Li,*[a] Xiaoning Li,[a] Hui-Ning Xiao,*[a, c] and Tony D. James*[b]

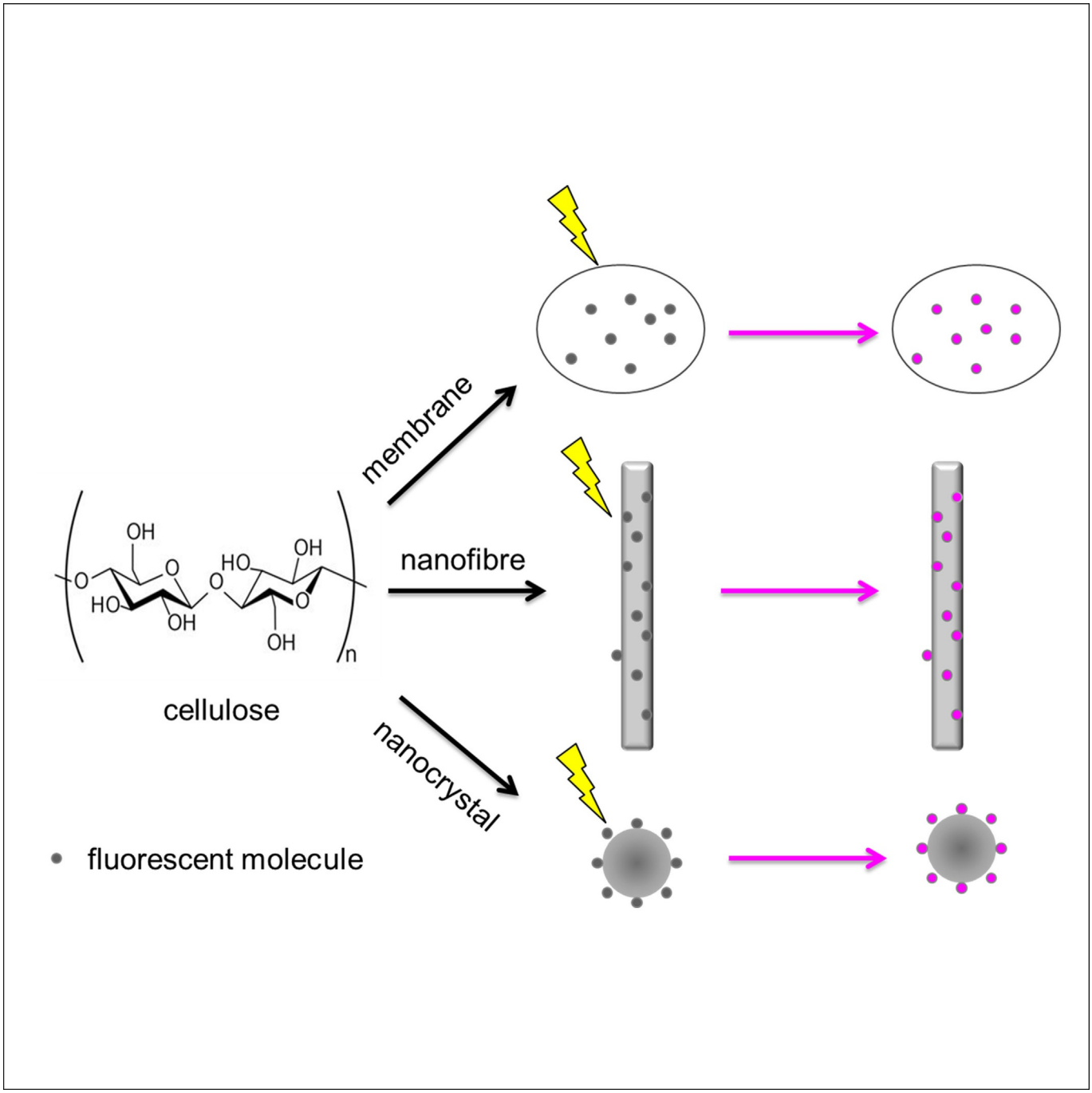

Cellulose-based materials functionalized with fluorescence sensors are highly topical and are employed in many areas of functional materials, including the sensing of heavy-metal ions and anions as well as being widely used as chemical sensors and tools for environmental applications. In this Review, we cover recent progress in the development of cellulose-based fluorescence sensors as parts of membranes and nanoscale materials for the detection of biological analytes. We believe that this Review will be of interest to chemists, chemical engineers, and biochemists in the sensor community as well as researchers working with biological material systems.

1. Introduction

Over several decades, fluorescence-based sensors have been extensively investigated owing to their high sensitivity and selectivity and the potential for rapid real-time monitoring of many analytes, including metal ions, nitrites, amino acids, and proteins.[1] With the development of sensing technology, conventional solution-based sensing has gradually shown limitations in real applications.[2] In comparison, solid-state sensor materials have some preferred advantages such as portability,[3] operational simplicity,[4] and reusability,[5] which make rapid online detection possible at a low cost.[6] These materials-based probes may be ultimately employed for basic laboratory assays as portable measurement devices and for household use as commercial indictors. Therefore, the quest for ecofriendly materials-based sensors with simple and smart detection is of exceptional importance.[7] Recently, intensive research has been devoted to the development of robust and highly selective and sensitive agents as replacements for conventional sensing molecules.[8] In this regard, cellulose materials such as membranes,[9] nanofibers,[10] and nanocrystals[11] serve as attractive probe candidates.

Cellulose is the most abundant organic material produced on the earth and approximately 5×10^{11} metric tons is generated yearly.[12] Cellulose is a colorless, odorless, and nontoxic solid polymer that possesses many promising properties, including biocompatibility, hydrophilicity, relative thermostability, high sorption capacity, and changeable optical appearance.[13] These properties enable cellulose to be applied in a vast number of fields.[14] Cellulose contains a number of hydroxy groups that can be used for functional-group modification, and this makes cellulose an excellent matrix for florescence-based sensing.[15] Thus, cellulose membrane and nanoscale fibers have been employed to fabricate fluorescent devices, as its nanoscale dimensions and its capacity to form a strong entangled nanoporous network encourage the emergence of new high-value applications.[16]

To the best of our knowledge, there are very few Reviews on fluorescent-sensing materials in which cellulose is used. Herein, we Review the preparation, properties, and applications of sensing materials based on cellulose developed over the last decade. We will introduce the fabrication strategies of fluorescence-based materials using cellulose as the main material or additive and focus on the properties of these materials and their potential applications (Scheme 1).

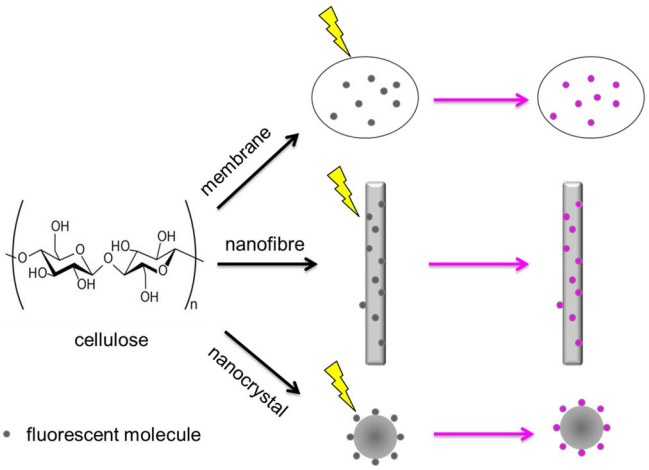

Scheme 1. Scheme of fluorescence-based sensing by using cellulose-based material supports.

2. Membrane-Based Fluorescent Cellulose

In most of the designs, optical chemical sensing is mainly performed with a chromophore immobilized in a polymer membrane. These types of sensing membranes display analyte-dependent optical properties such as absorbance and fluorescence. Mostly, such sensors provide enhanced stability, reversibility, and sensitivity with respect to solution-based sensing systems.

2.1. Electrospun Nanofibrous Membranes

Electrospinning is a remarkably simple and versatile technique capable of generating continuous nanofibers directly from a

[a] *Dr. M. Li, X. Li, Prof. H.-N. Xiao*
Department of Environmental Science and Engineering
North China Electric Power University
689 Huadian Road, Baoding, 071003 (P. R. China)
E-mail: mlincepu@hotmail.com

[b] *Prof. T. D. James*
Department of Chemistry, University of Bath
Claverton Down, Bath, BA2 7AY (UK)
E-mail: t.d.james@bath.ac.uk

[c] *Prof. H.-N. Xiao*
Department of Chemical Engineering, University of New Brunswick
Fredericton, NB, E3B 5A3 (Canada)
E-mail: huiningxiao@hotmail.com

The ORCID identification number(s) for the author(s) of this article can be found under:
https://doi.org/10.1002/open.201700133.

variety of polymers and composite materials. Owing to its high porosity and large specific surface area, an electrospun functional polymer nanofibrous membrane can serve as an ideal scaffold for sensor applications.

Liu and co-workers[17] report a simple method to fabricate fluorescent nanofibers by using the electrospinning technique with fluorophore-doped polymers (Figure 1). 9-Chloromethylanthracene (9-CMA) is used as the fluorophore to be doped into the host matrix network of cellulose acetate. The sensing performance of the nanofiber membrane is evaluated by its quenching behavior towards methyl violet. Importantly, the sensing behavior is substantially improved by introducing secondary porous structures into the nanofibers, which are introduced by a porogen or deacetylation treatment. In addition, the prepared nanofibrous membranes display excellent stability, reusability, and reproducibility with no fluorophore leakage, and they are suitable for sensing water-soluble species. It is clear that the strategy for fabricating secondary porous structures will enrich this research area and improve the development of sensors based on electrospun nanofibrous membranes.

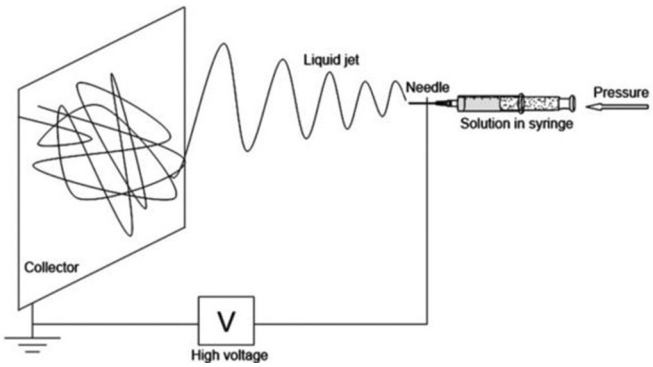

Figure 1. Schematic illustration of the electrospinning setup. Reproduced from Ref. [17] with permission of the Royal Society of Chemistry.

Recently, Ongun and co-workers[18] have reported a method to combine nanoscale electrospun fiber materials with fluores-

Meng Li is now a lecturer at the North China Electric Power University (Baoding). She obtained her B.Sc. degree in 2011 (East China University of Science and Technology) and was then a combined Master's/Ph.D. student from 2011 to 2012 (with Prof. Weihong Zhu in China) and then worked with Prof. Tony D. James for her Ph.D. degree at the University of Bath from October 2012 to July 2015. She obtained a Global Research Scholarship from the University of Bath during her study and visited Ewha Womans University in South Korea (and worked with Prof. Juyoung Yoon) for 2 months starting in March 2015. Her research interests comprise many aspects of supramolecular chemistry, electrochemistry, and materials chemistry, including molecular recognition, electrochemical sensing, and the fabrication of materials.

Xiaoning Li is a Master's degree candidate at the North China Electric Power University. She obtained her bachelor's degree from Hebei University of Engineering in 2016 and majored in Water Supply and Drainage. From 2016 to now, her research interests have focused on cellulose materials for sensing and the adsorption of heavy metals.

Hui-Ning Xiao is a Professor in Chemical Engineering at the University of New Brunswick (UNB) in Fredericton, NB, Canada, and is a Fellow of the Canadian Academy of Engineering. He obtained his B.Eng./M.Eng. degrees from Nanjing University of Technology in 1982/1987 and his Ph.D. degree from McMaster University in 1995. He took a post as Lecturer at the University of Manchester (formerly UMIST) in 1996. Since joining the UNB in 2001, he has attracted substantial research funding from various sources. He was the team leader for two NSERC strategic networks: sentinel-bioactive paper and innovative green wood fiber products. He has extensive research experience in developing polymers/nanoparticles for green-based materials and functional modification of cellulose fibers. To date, he has published over 210 SCI peer-reviewed journal papers.

Tony D. James is a Professor at the University of Bath and a Fellow of the Royal Society of Chemistry and holds a prestigious Royal Society Wolfson Research Merit Award (2017–2021). He obtained his B.Sc. degree from UEA in 1986, his Ph.D. degree in 1991 from the University of Victoria, and worked as a PDRF in Japan from 1991 to 1995 with Seiji Shinkai. From 1995 to 2000, he was a Royal Society Research Fellow at the School of Chemistry at the University of Birmingham and moved to the Department of Chemistry at the University of Bath in September 2000. His research interests focus on the use of boronic acid based receptors for the fluorescence sensing of saccharides.

cent molecules for Cu^{II} sensing (Figure 2). In this work, poly(methylmethacrylate) (PMMA) and ethyl cellulose(EC) are employed as the polymeric support materials to fabricate the fluorophore: *N*′-3-[4-(dimethylaminophenyl)allylidene]isonicotinohydrazide. The sensor membranes exhibit excellent sensitivity owing to the high surface area of the nanofibrous membrane structures, and the sensitivity is 6–20 times higher than that for continuous thin films. These sensor membranes achieve the largest reported working ranges and the best limits of detection among similar emission-based sensing methods for a concentration range of 10^{-12} to 10^{-5} M for Cu^{2+}. The authors aim to explore new sensing materials and polymer compositions by controlling the size of the electrospun membranes and by optimizing the sensitivities for the detection of analytes.

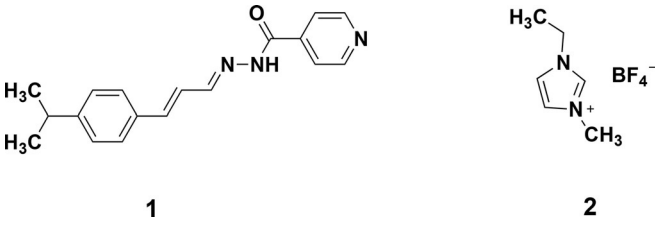

1 2

Figure 2. Structures of the Cu^{2+}-sensitive fluoroionophores: *N*′-3-[4-(dimethylaminophenyl)allylidene]isonicotinohydrazide (DPAINH, **1**), 1-ethyl-3-methylimidazolium tetrafluoroborate (EMIMBF 4, **2**).

Min and co-workers[19] have developed an approach to construct a Cu^{2+} sensor based on electrospun rhodamine-dye-doped poly(ether sulfone) (PES) nanofibers. In Figure 3, the film produces a significant color change from white to pink, and this color change confirms that Cu^{2+} induces ring opening of the spirolactam moiety in the rhodamine dye. The nanofibrous sensor displays good sensitivity, selectivity, and reusability toward Cu^{2+}, and the limit of quantification (LOQ) is 1.1×10^{-9} M. In addition, the authors propose a 1:1 complex stoichiometry for the rhodamine dye and Cu^{2+}. Furthermore, the nanofibrous sensors can be reused conveniently to achieve practical sensing in aqueous medium just like using a test paper, and other metal ions show almost no interference. More importantly, this method allows expansion of the range of target analytes simply by changing the fluorescent probe. Compared to small-molecule chemosensors, nanofibrous sensors represent a simple and applicable strategy for the practical detection of heavy-metal ions in the environment. Niu and co-workers[20] have synthesized a cellulose nanofibrous film by grafting a boronate-terminated conjugated polymer (CP) with the C-6 carboxy groups of a cellulose nanofiber (CNF) film surface (Figure 4). The sensing performance of the PFC@CNF (PFC = boronate-terminated conjugated polymer chains) films

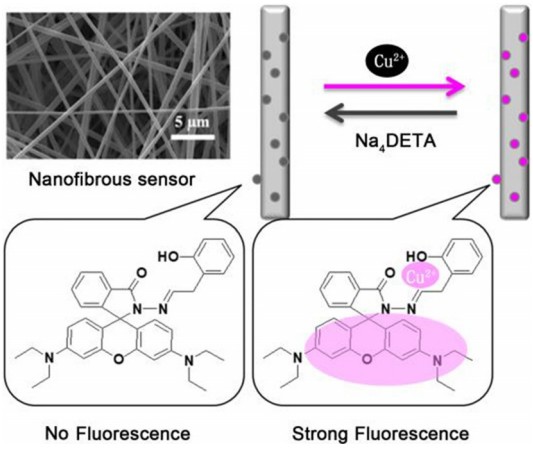

Figure 3. Schematic illustration of the Cu^{2+} sensing of rhodamine-dye-doped PES nanofibrous sensor; Na_4DETA = tetrasodium ethylenediamine tetraacetic.

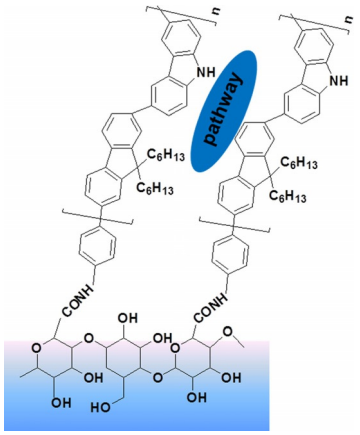

Figure 4. Schematic of the route for the synthesis of the PFC@CNF film.

is evaluated by fluorescence quenching in the detection of nitroaromatic vapors [2,4-dinitrotoluene (DNT) and 2,4,6-trinitrotoluene (TNT) are used as representative nitroaromatics]. The fraction of easily accessible cavities of the novel fluorescent film sensor reaches up to 0.97, and relative to the SC(FC) film and FC@CELL paper, it exhibits enhanced response toward DNT vapor. By examining the sensing process with DNT vapor as a representative nitroaromatic, the PFC@CNF films display efficient quenching and recovery. In addition, the film is stable to photobleaching and has good reversibility and good fluorescence stability.

Kacmaz and co-workers[21] propose the fabrication of nanofibrous mats and continuous thin films by electrospinning and knife-spreading techniques, respectively. Probe **3** has been chosen as the fluorescence probe for doping of the polymeric ethyl cellulose (EC) matrix material together with an ionic liquid (Figure 5). The sensors characteristics have been extensively investigated, including response time, reversibility, linear working range, effect of pH, and interference effect, and these sensors display high selectivity and sensitivity to Cu^{2+} ions in the presence of other ions. Moreover, the novel nanofiber displays a sensitive response with a detection limit of

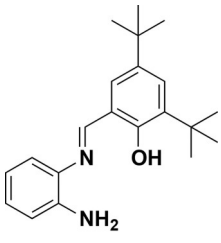

3

Figure 5. Structure of copper-sensing fluoroionophore **3**.

3.3×10^{-13} M towards Cu^{2+} ions over a wide range of concentrations (i.e. 5.0×10^{-12} to 5.0×10^{-5} M). Furthermore, the fiber-optic sensor system exhibits high sensitivity and excellent selectivity for the detection of Cu^{II} at the picomolar level.

Very recently, an attempt has been made to develop a simple sensor strip for the detection of lead (Pb^{2+}) by the electrospinning method.[22] The novel nanofibers (NFs) use curcumin-loaded cellulose acetate (CC-CA), and upon exposure to Pb^{2+}, these nanofibers display a visual color change from yellow to orange over a concentration range of 10 nM to 1 mM. This method has many advantages, including low cost, convenience, biocompatibility, and sensitivity for the quantitative detection of Pb^{2+} with a low detection limit of 20 μM. In Figure 6, the nanofibrous membranes are capable of determining Pb^{2+} ions with a high selectivity over other ions. In addition, the authors propose the use of curcumin nanofibers to detect lead ions, and the results are promising for the development of low-costing disposable sensors for rapid and real-time applications.

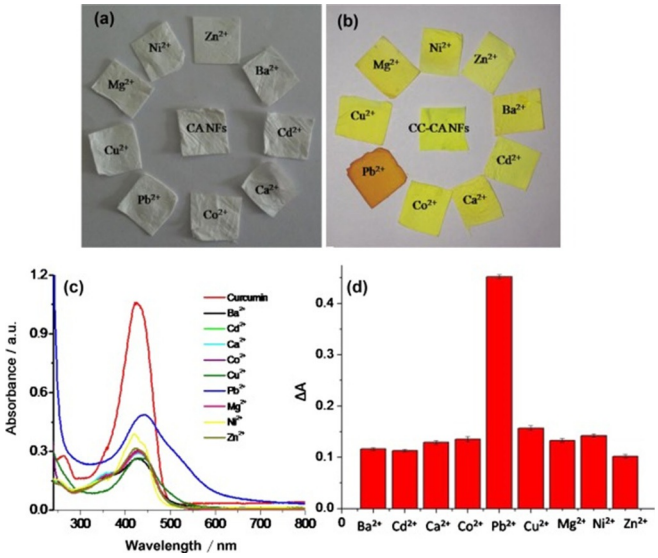

Figure 6. Selectivity of Pb^{2+}; a) selectivity of Pb^{2+} by using a curcumin-free CA nanofiber membrane. b) Selectivity of the CC-CA nanofiber membrane upon contact with various metal ions. c) UV/Vis absorption spectra for the selectivity to Pb^{2+} in the presence of various metal ions. The concentration of the metal ions was 1000 μM for Ba^{2+}, Cd^{2+}, Ca^{2+}, Co^{2+}, Pb^{2+}, Cu^{2+}, Mg^{2+}, Ni^{2+}, and Zn^{2+}. d) Bar chart of the CC-CA membrane for various heavy-metal ions. Reproduced from Ref. [22] with permission of Elsevier.

2.2. Filter-Paper-Based Fluorescence Sensors

Filter paper is another ideal support for sensor applications. Recently, Zhang and co-workers[23] have reported a method to fabricate a chemosensor for the detection and adsorption of Hg^{2+} ions in aqueous media. As shown in Figure 7, the coating of ruthenium dye N719 [ditetrabutylammonium *cis*-bis(isothiocyanato)bis(2,2′-bipyridyl-4,4′-dicarboxylato)ruthenium(II)] is chosen as the fluorophore to be doped into the host matrix network of titania-precoated cellulose nanofibers of a bulk natural cellulose substance (filter paper). The chemosensor exhibits high selectivity, sensitivity, and reversibly, and it also shows excellent absorption ability as a result of its high surface area. Moreover, the limit of detection is about 10 ppb. This methodology for the fabrication of sensing materials introduces a new strategy for the detection and adsorption of heavy-metal ions from aqueous media suitable for practical applications.

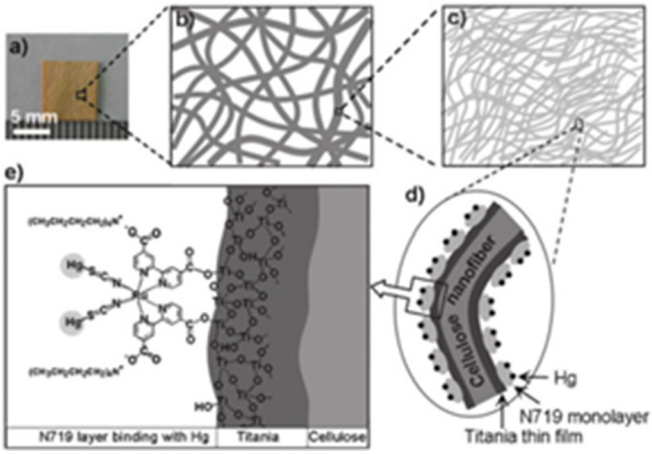

Figure 7. Schematic representation of Hg^{2+} sensing by using titania/N719 multilayer modified natural cellulose substance (common commercial filter paper). Reproduced from Ref. [23] with permission of the Royal Society of Chemistry.

Xu and co-workers[24] have developed a solid-state sensor for the detection of Hg^{2+} ions in aqueous media that is based on a rhodamine-modified cellulose filter paper (Figure 8). A spirolactam rhodamine derivative is utilized, and its transformation into the ring-opened form produces a rapid and specific fluorescence turn-on response. This solid-state sensor exhibits selective recognition and fast response towards Hg^{2+} ions in a Tris-HNO_3 buffer solution (pH 7.24) and is unaffected by a background of other environmentally relevant metal ions. Furthermore, the simple solid-state sensor has been used for the col-

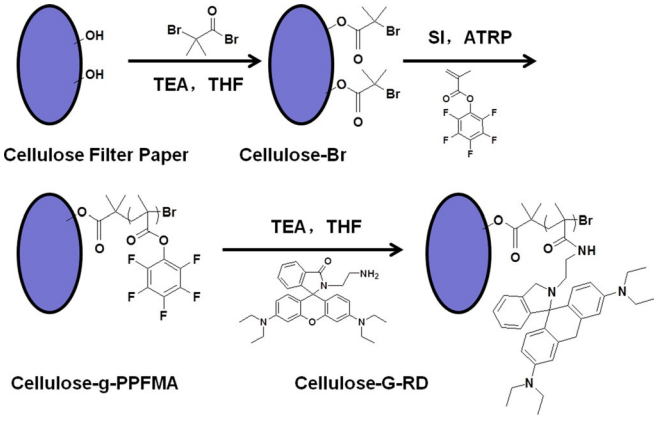

Figure 8. Diagram illustrating the reaction of the hydroxy groups of the cellulose filter paper with 2-bromoisobutyrate bromide to produce alkyl-halide-immobilized cellulose-Br, surface-initiated ATRP (SI-ATRP) from cellulose-Br to produce poly(pentafluorophenyl methacrylate) (PPFMA)-grafted filter paper (cellulose-g-PPFMA), and postfunctionalization of reactive cellulose-g-PPFMA with amino-containing spirolactam rhodamine derivatives to produce a rhodamine-derivative-modified cellulose filter paper (cellulose-g-RD). TEA = triethylamine.

orimetric and fluorescence detection of Hg^{2+} ions in aqueous media, with enhanced fluorescent emission intensity and distinct color change from colorless to pink. The disposable solid-state sensor can be applied in many practical applications for the detection of environmental and biological Hg^{2+} ions. Liu and co-workers[25] report on a fluorescent silver nanocluster (AgNC)-based sensor (Figure 9). These water-soluble AgNCs

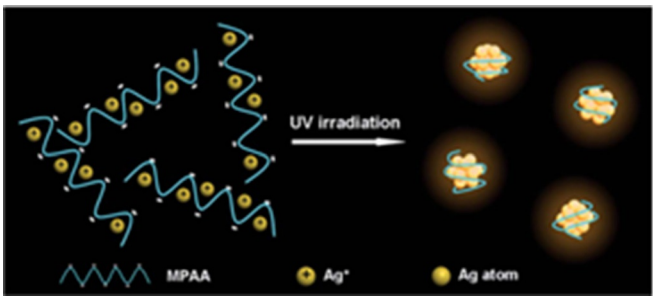

Figure 9. Illustration of the direct synthesis of AgNCs by using modified poly(acrylic acid) (MPAA) as a template. Reproduced from Ref. [25] with permission of the Royal Society of Chemistry.

have been chosen as a new class of fluorescence probes for deposition onto cellulose paper. The sensing performance of the novel sensor has been evaluated through its fluorescence quenching by Cu^{2+} ions. The sensor displays good selectivity toward Cu^{2+}, and the Cu^{2+} response is hardly affected by competitive metal ions. This work improves current approaches for Cu^{2+} detection and provides the potential for the development of robust cluster-based sensing platforms.

Chen and co-workers[26] have developed a colorimetric sensing strategy by combining unmodified gold nanoparticles (AuNPs) and microfluidic paper-based analytical devices (μPADs) for Hg^{2+} monitoring (Figure 10). The method uses a portable and cost-effective toolset instead of expensive materials or complicated preparation processes for Hg^{2+} detection in resource-constrained settings. The system shows high specificity toward Hg^{2+}, even if the concentrations of other metal ions are 10-fold higher than the concentration of Hg^{2+} in aqueous solution. A detection limit of 50 nM for Hg^{2+}-spiked pond and river water is obtained. In addition, the μPAD can incorporate other nanomaterial-based heavy-metal sensors for simultaneous detection of different metal ions in a single pot for environmental pollution control and monitoring.

Núñez and co-workers[27] have reviewed a method to fabricate two new rhodamine-based chemosensors by using low-costing simple cellulose discs. Rhodamine B or the rhodamine 640 moiety is used to synthesize two novel probes, **4** or **5**, for Hg^{2+} (Figure 11). The performances of **4** and **5** have been evaluated and both display remarkably high selectivity for Hg^{2+} with a low detection limit for Hg^{+} (1.5 ppm for **4** and 3.4 ppm for **5**; signal-to-noise ratio of 3:1). In addition, a color

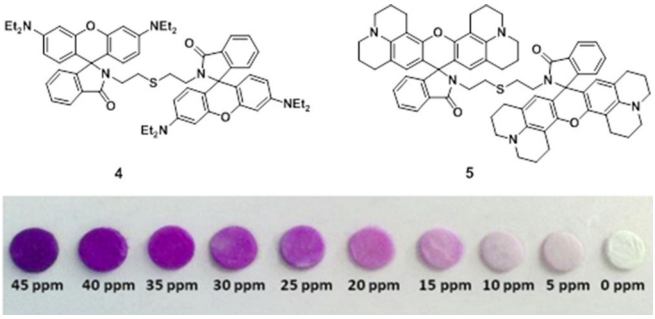

Figure 11. Chemical structures of compounds **4** and **5** and visual changes of blank discs (Liofilchem) containing compound **4** (2.00×10^{-9} mol) after immersing (5 s) in water solutions (pH 6.9–7.2) containing increasing amounts of Hg^{2+} (0–45 ppm). Reproduced from Ref. [27] with permission of Elsevier.

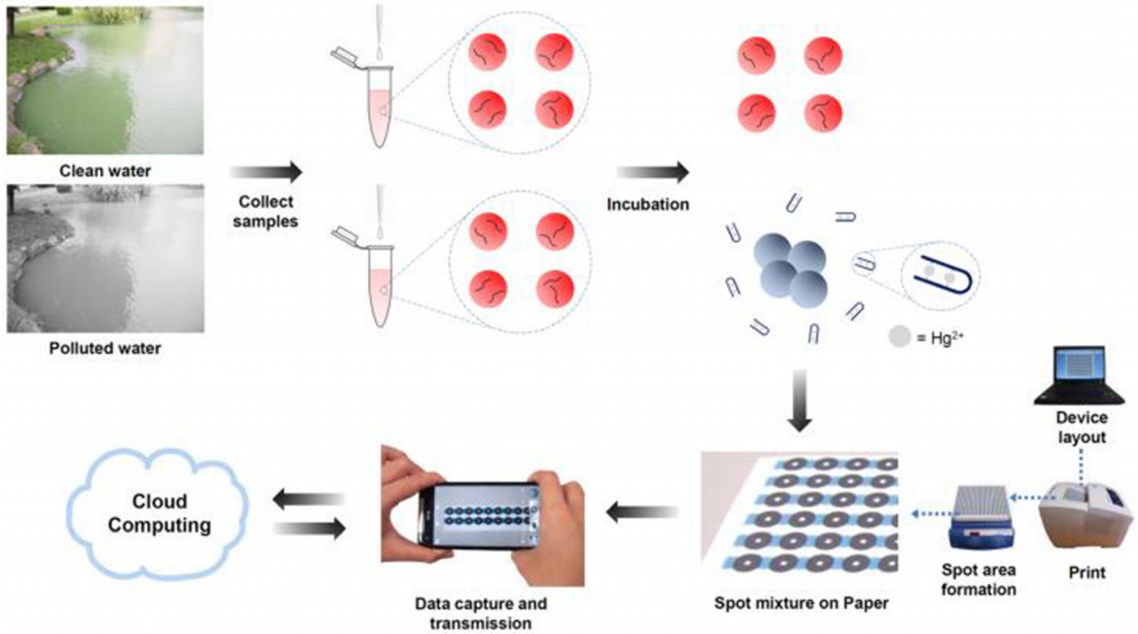

Figure 10. Illustration of proposed on-site Hg^{2+} sensing. Reproduced from Ref. [26] with permission of the American Chemical Society.

change from colorless to pink is observed in both cases with an increase in the absorption and emission signals. Sensors **4** and **5** can be used for the detection of Hg^{2+} ions in both aqueous solution and in the gas phase.

Srivastava and co-workers[28] have designed and synthesized an efficient photoinduced electron-transfer (PET) fluorescence probe. An anthracene moiety is used as a fluorescent signaling unit that is introduced into an ionophore consisting of benzhydryl moieties and piperazine units. The addition of Hg^{2+} ions results in a significant fluorescence enhancement (≈10-fold). Moreover, in Figure 12, it can be seen that the blue color of

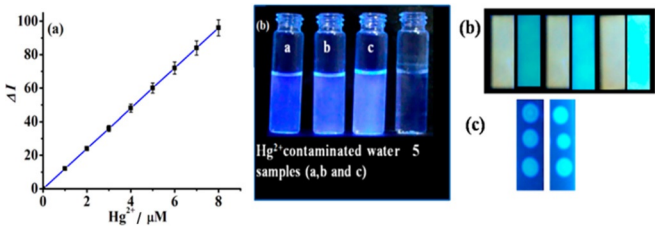

Figure 12. a) Calibration sensitivity plot of the probe for Hg^{2+} and b) change in color of probe and probe + Hg^{2+} solution ($a = 0.02$, $b = 0.2$, $c = 2$ μM) in 4-(2-hydroxyethyl)-1-piperazineethanesulfonic acid (HEPES) buffer and change in color of probe and probe + Hg^{2+} on c) cellulose paper strips and d) silica-coated slides. Reproduced from Ref. [28] with permission of the American Chemical Society.

the solution changes to blue-green (switched-on), as viewed by the naked eye. The probe displays good linear and real-time fluorescence "turn-on" response in addition to high sensitivity and selectivity for the detection of Hg^{2+} ions in partial aqueous medium, in real water samples, and on cellulose paper strips and silica coated microslides. Moreover, the detection limit of 2 ppb with recovery in the range of 90 to 115% indicates that the system has great potential for the detection of Hg^{2+} ions in real biological and environmental samples.

A smart sensor device has been developed by Rull-Barrull et al.,[29] who grafted a rhodamine sensor onto a highly hydrophilic surface of paper. This system has been used for the colorimetric and optical detection of hydrogen sulfate in water. Furthermore, the solid-state sensor has been used to detect HSO_4^- ions in aqueous media, with enhanced fluorescent emission intensity and a distinct color change from colorless to pink (Figure 13). It displays high selectivity and a limit of detection over the range of 0.1 to 0.5 mM, as view by the naked eye, and is not affected by the presence of other anions. In addition, this practical technology can be used in environmental and analytical sciences. Currently, the diversification of this technology is being investigated for the sensing of other liquid and gas analytes.

A one-step hydrothermal method developed by Bian and co-workers[30] allows the production of cellulose-based fluorescence materials by loading ZnS quantum-dot-decorated graphene directly onto the surface of paper fibers (Figure 14). The composite exhibits only a fewer defects and high fluorescence intensity. Given that the fluorescent color of this cellulose-based material can be regulated by doping different heteroatoms into ZnS, there is great potential for this material to be used in flexible photocatalytic materials, luminescent materials, and nanoscale photosensor applications.

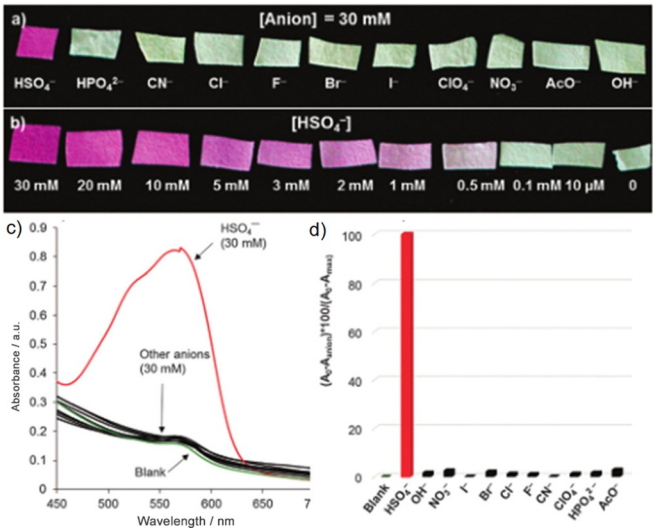

Figure 13. a) Colorimetric detection of tetrabutylammonium salts in water at 30 mM by simple naked-eye analysis of the dipped paper strip. b) Effect of the concentration of HSO_4^- anions on the color change of the paper strip. c) UV/Vis absorption spectra of the paper strip dipped into aqueous solutions of HSO_4^-, HO^-, NO_3^-, I^-, Br^-, Cl^-, F^-, CN^-, ClO_4^-, HPO_4^{2-}, and AcO^- at 30 mM. d) Normalized absorbance response of the paper strip. Reproduced from Ref. [29] with permission of the Royal Society of Chemistry.

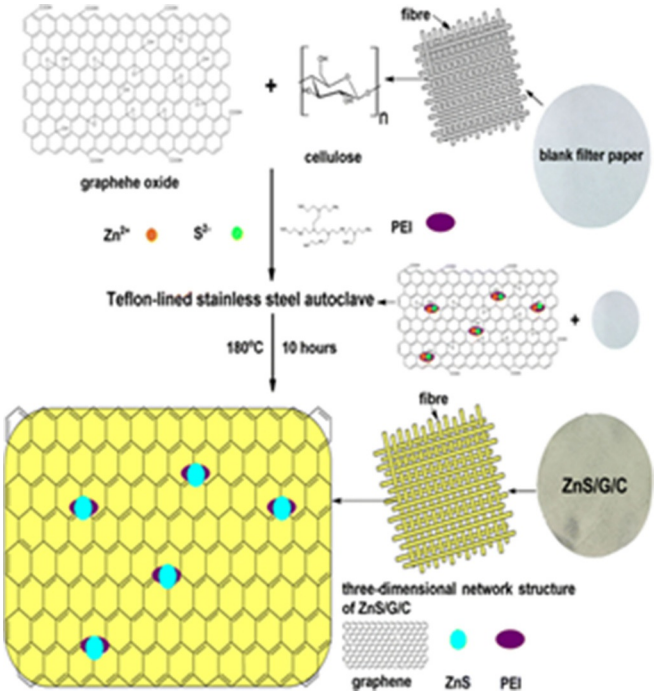

Figure 14. Fabrication procedure of cellulose-based composite ZnS/graphene (G)/cellulose (C); PEI = polyethylene mine. Reproduced from Ref. [30] with permission of Springer.

2.3. Other Membrane Applications

Recently, Veciana and co-workers[31] have developed a novel method for the fabrication of a solid-state membrane filter by filtering nanoparticles of a fluorophoric mercury(II) sensor dispersed in water through a nanopore-sized cellulose membrane. 1-(4′-Methoxyphenyl)-4-(1′-pyrenyl)-2,3-diaza-1,3-butadiene is a fluorescent and highly selective mercury sensor that is loaded onto the membrane fibers to produce a nanocomposite membrane (Figure 15). The novel membrane exhibits excellent selectivity and high sensitivity down to trace levels. The method involving the use of nanocomposite membranes for the detection of mercury(II) ions in water has proven to be particularly advantageous for environmental detection.

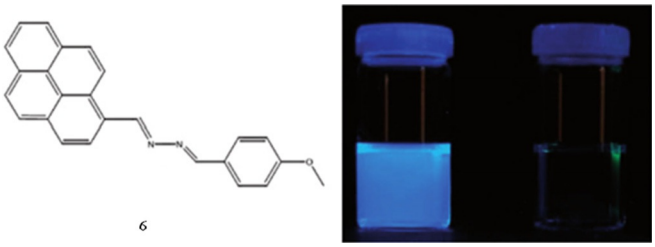

Figure 15. Left) Molecular structure of the unsymmetrical azine. Right) Fluorescence emission from an aqueous solution (CH_3CN/H_2O, 7: 3) of the mercury molecular probe with Hg^{2+} (6 equiv.) and without Hg^{2+} ions. Reproduced from Ref. [31] with permission of the Royal Society of Chemistry.

Duong and Rhee[32] have developed a ratiometric fluorescence urea biosensor. The perchlorate (O17)–ethyl cellulose (EC) membrane and a layer of the urease enzyme are immobilized in an ethyl cellulose matrix. The properties of the urea-sensing membrane have been investigated towards concentrations of urea with limit of detection (LOD) values of 0.027 and 0.224 mM in the ranges of 0.01 to 0.1 M and 0.1 to 1.0 M, respectively (Figure 16). The system exhibits a fast response time, high reversibility, and long-term stability over these concentration ranges. Moreover, the urea-sensing membrane shows excellent reproducibility with a very low relative standard deviation (less than 3%). This system will be particularly useful in clinical chemistry as well as in food chemistry and environmental monitoring owing to its high level of recovery.

Campos and co-workers[33] have proposed a highly hydrophilic planar membrane by using a simple and chemically friendly technique. Both bare silicon quantum dots (SiQDs) and SiQDs coated with a polyamidoamine dendrimer with hydroxy surface groups (PAMAM-OH) are introduced into a support membrane of a regenerated cellulose (RC-4 membrane) (Figure 17). Both of the SiQDs–regenerated cellulose composite membranes have luminescent properties, and relative to the original sample, they have higher thermal resistance and conductivity. The QD-modified cellulose supports have been characterized electrochemically by using KCl solutions at different concentrations. These stable nanoengineered biocompatible membranes based on SiQD nanoparticles with luminescent properties have great potential in flow devices.

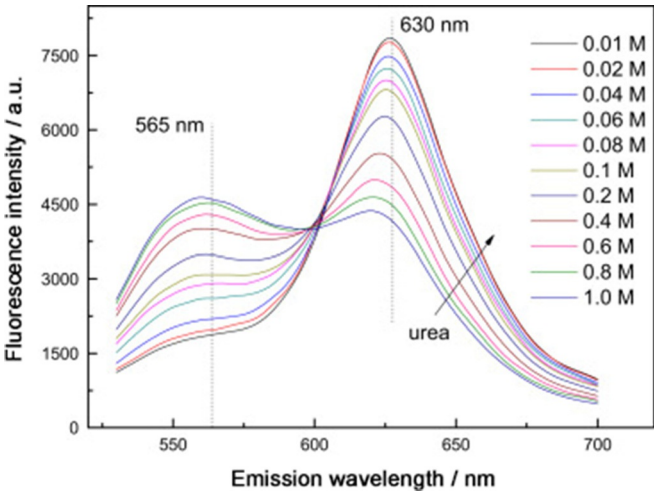

Figure 16. Fluorescence emission spectra of the urea-sensing membrane to urea concentrations in the range of 0.01 to 1.0 M, as monitored at an excitation wavelength of 470 nm. Reproduced from Ref. [32] with permission of Elsevier.

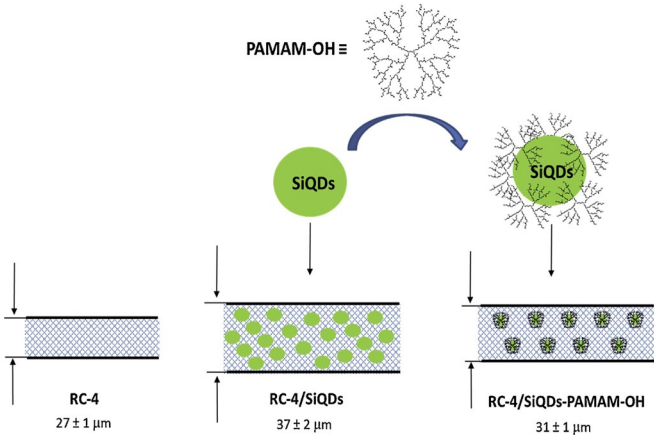

Figure 17. Schematic representation of the RC-4 membrane and the modified RC-4/SiQDs and RC-4/SiQDs-PAMAM-OH membranes, as well as indication of their average thickness. Reproduced from Ref. [33] with permission of Elsevier.

3. Nanoscale Fluorescent Cellulose

On the basis of construction strategies for functional nanomaterials, this section REVIEWs polysaccharide nanocrystal-based functional nanomaterials with sensing applications.

3.1. Nanofiber-Based Fluorescence Sensors

A novel solid-state fluorescence biosensor reported by Davis and co-workers[34] is prepared by the electrospinning method. An ionic fluorescent dendrimer (AFD) is encapsulated into celluloseacetate (CA) nanofibers for the detection of metalloproteins by a quenching mechanism. Importantly, to realize enhanced molecular interactions it is desirable to introduce secondary porous structures into the nanofibers generated by the deacetylation of cellulose. Scheme 2 outlines the electrospinning setup, encapsulation of the fluorescent dendrimer, and

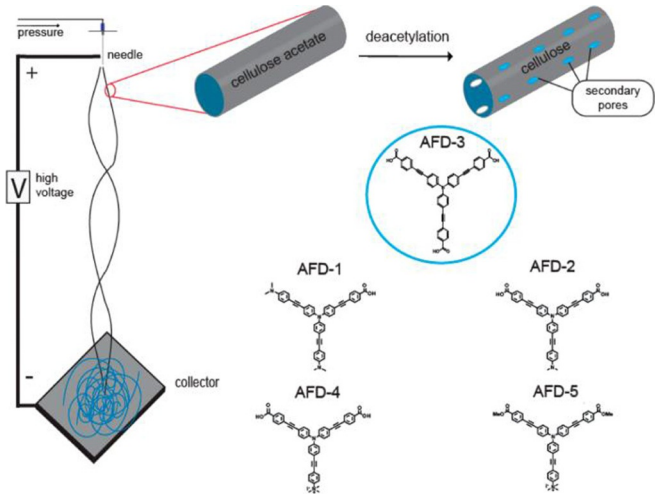

Scheme 2. Schematic illustration of the electrospinning setup, encapsulation of the fluorescent dendrimer, and deacetylation process used in this study; five water-soluble fluorescent dendritic compounds (i.e. AFD-1, AFD-2, AFD-3, AFD-4, and AFD-5) composed of phenylene–ethynylene repeating units are illustrated. Reproduced from Ref. [34] with the permission of the American Chemical Society.

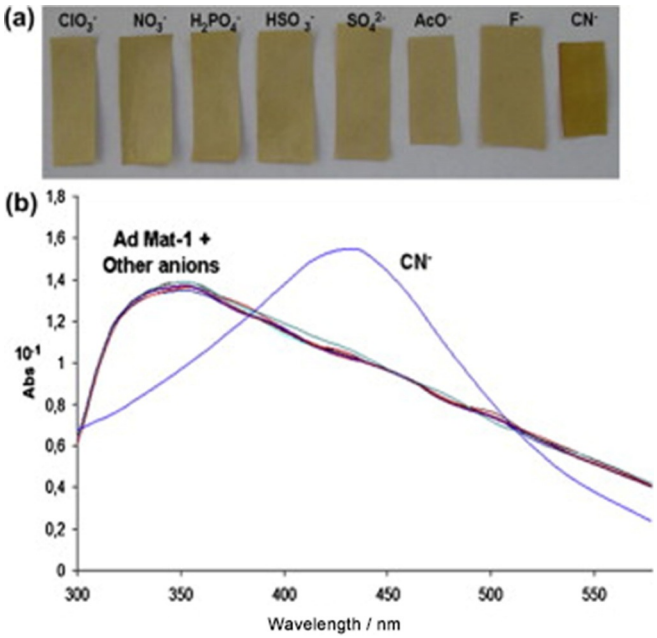

Figure 18. a) Color change in the chemosensor-modified cellulose fiber upon exposure to 1 mM aqueous solutions of different anions. b) Solid UV/Vis spectra of the chemosensor azo-dye-modified cellulose fiber after dipping in aqueous solutions at pH 7 with different anions. Reproduced from Ref. [35] with permission of Elsevier.

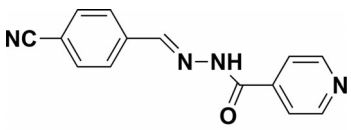

7

Figure 19. *N*′-(4-Cyanobenzylidene) isonicotinohydrazide (CBINH).

the deacetylation process. The biosensor exhibits better reproducibility, reversibility, and durability than the non-encapsulated nanofibers owing to the large surface area of the former. In addition, nanofiber sensor arrays containing different fluorescent dendrimers will be prepared for the detection and identification of protein targets through distinct fluorescence response patterns.

Isaad and Achari[35] have developed dye-sensitized cellulose materials by introducing two new water-soluble azo dyes into cellulosic fibers for the detection of cyanide anions in aqueous media. Owing to the high surface areas of the functionalized cellulose material, as displayed in Figure 18, cyanide ions induce a color change from green/yellow to yellow/orange, whereas no change is observed in the presence of other anions. As expected, these easy-to-use materials also demonstrate high selectivity in aqueous solution over other anions with detection down to 0.01–0.07 mM for the cyanide anion.

Sibel and co-workers[36] have fabricated ethyl cellulose (EC)-based nanofibers by using an electrospinning technique. As shown in Figure 19, *N*′-(4-cyanobenzylidene)isonicotinohydrazide (CBINH, **7**) acts as the indicator, and it is doped into a polymeric matrix of EC nanofibers for the optical sensing of Fe^{3+}. These nanofibers achieve fast response times of less than 30 s, which is faster than the response times of similar solid-state sensing agents. Over a wide concentration range (1.0×10^{-12} to 1.0×10^{-6} M), the nanofibers exhibit excellent sensitivity and selectivity with a detection limit of 0.07 pM for Fe^{3+} ions. Additionally, the nanostructures provide faster sensor dynamics in practical applications.

Ikai et al.[37] have reported a chiral fluorescence sensor, designed and synthesized from naturally occurring optically active cellulose. The novel cellulose derivative bearing π-conjugated terthienyl pendants is used as a fluorescent signaling unit. The chiral recognition abilities have been investigated on the basis of an enantioselective fluorescence response to optically active aromatic nitro compounds containing central and axial chirality (Figure 20). It is anticipated that polysaccharide-based chiral fluorescent sensors with superior enantioselectivity can be developed by an appropriate selection of polysaccharide backbones and structural modification of the fluorescent pendants.

Xiong and co-workers[38] have prepared fluorescent lignin nanoparticles by using a combination of alkoxysilane chemistry, amidation, and sonication. 1-Pyrenebutyric acid (PBA) acts as the fluorescence probe, and it is grafted onto the lignin surface by amidation, as shown in Scheme 3. Oxygen quenches the fluorescence of the lignin–PBA. Furthermore, with an increase in the PBA concentration, the sensitivity to oxygen is enhanced. Owing to its high sensitivity and rapid response towards oxygen molecules, the fluorescent lignin can potentially be employed as an oxygen sensor.

Yang and co-workers[39] have developed novel S-doped carbon quantum dots (S-CQDs) that are fabricated from cellulose fibers as the carbon precursor and sulfuric acid as the carbonization agent and dopant. More importantly, as can be seen in Figure 21, the S-CQDs demonstrate excellent selectivity and sensitivity and can be utilized to detect Fe^{3+} in pH 0 solu-

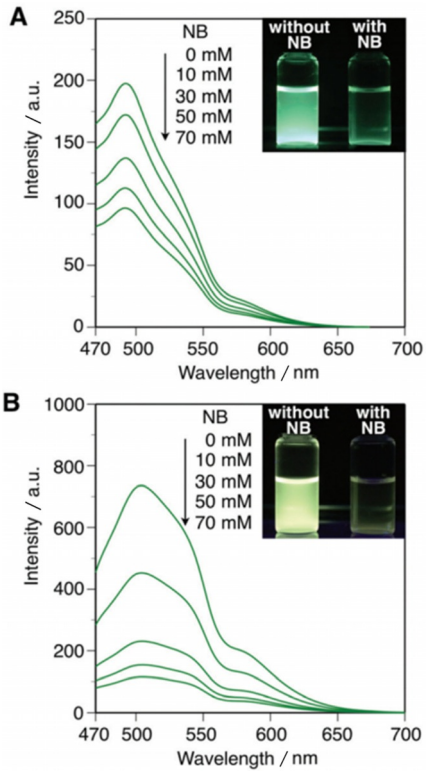

Figure 20. Fluorescence spectra upon the addition of various amounts of nitrobenzene (0–70 mM) in a) THF and b) hexane/THF (90:10 *v/v*) at RT. [Glucose unit] = 1.0×10^{-5} M. Inset) Photographs of the solutions in the absence (left) and presence (right) of nitrobenzene (70 mM) under irradiation at $\lambda = 365$ nm. Reproduced from Ref. [37] with permission of the Royal Society of Chemistry.

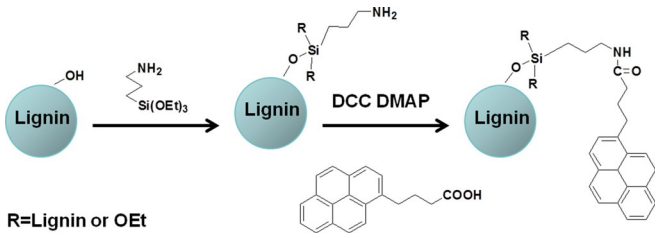

Scheme 3. Schematic illustration of the fluorescent functionalization of lignin. DCC = *N,N'*-dicyclohexylcarbodiimide, DMAP = 4-dimethylaminopyridine.

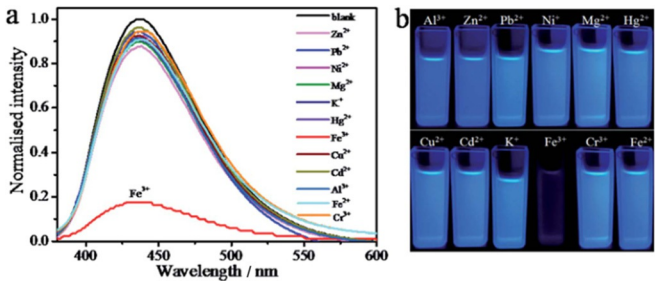

Figure 21. a) Photoluminescence spectra of S-CQDs dispersed in pH 0 aqueous solutions with 2 mM of different ions and b) the corresponding pictures. Reproduced from Ref. [39] with permission of the Royal Society of Chemistry.

tions with a detection limit of 0.96 μM. In this acidic environment (pH 0), the S-CQDs also exhibit strong, stable, and excitation-independent fluorescence emission with a high quantum yield (up to 32%) and extremely acidophilic high luminescence. In addition, the method used to fabricate the S-CQDs provides a foundation for the development of CQD sensors that can be used under strongly acidic conditions.

3.2. Nanocrystal-Based Fluorescence Sensors

Qiang and Pan[40] have developed a unique and simple method for the preparation of fluorescent cellulose nanocrystals (CNCs) by a two-step approach. Scheme 4 shows that in

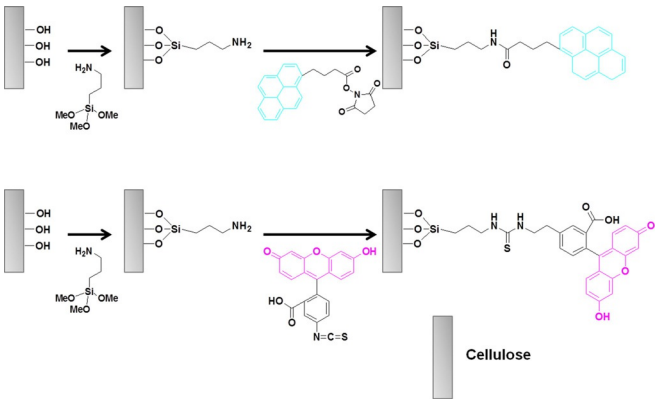

Scheme 4. Schematic illustration of the fluorescent functionalization of cellulose.

the first step reactive amino groups are introduced into the cellulose surface through a silanization reaction. This is followed by fluorescent functionalization by using 1-pyrenebutyric acid *N*-hydroxysuccinimide ester (PSE) or fluorescein isothiocyanate (FITC). Furthermore, this approach can be successfully applied to other cellulose materials containing CNCs, microcrystalline cellulose (MCC), and bulky paper sheets. Therefore, these fluorescence-based cellulose materials have great potential in functional papers, sensors, and bioimaging applications.

Edwards and co-workers[41] have outlined an approach involving the use of cotton cellulose nanocrystalline (CCN) fluorescent peptide conjugates as a sensitive biosensor for human neutrophil elastase (HNE) and porcine pancreatic elastase (PPE). Figure 22 shows the chemical structures of the peptide–cellulose conjugates. Relative to that shown by the tripeptide, the tripeptide–CCN conjugate displays efficiency for HNE in solution that is fivefold greater, as judged by a k_{cat}/K_m value of 33515. At a loading of 2 mg of the tripeptide– and tetrapeptide–CCN conjugates over a reaction time of 10 min, as monitored by a change in the fluorescence, the limits of detection of the sensors are 0.03 U mL^{-1} for PPE and 0.05 U mL^{-1} for HNE, respectively. Importantly, this elastase biosensor demonstrates interesting activity and structural properties.

Recently, Chen and co-workers[42] developed cellulose nanocrystalline (CNC)–poly(amidoamine) (PAMAM) materials. G6-

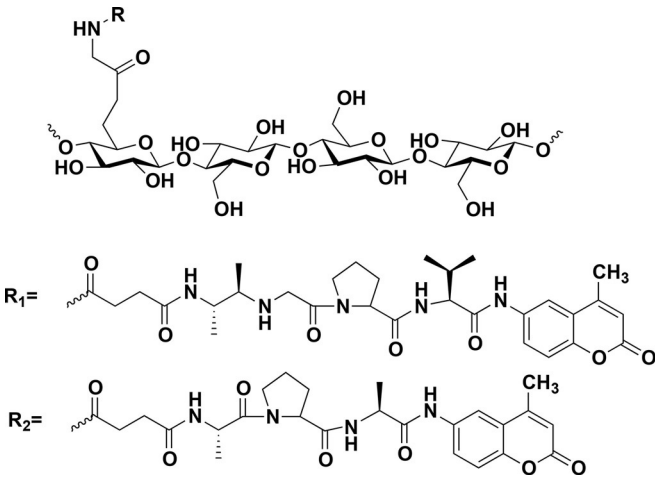

Figure 22. Structures of CCN–(O–C(O) Gly-NHC(O))succinyl-Ala-Ala-Pro-Val-AMC (R^1 analogue) and CCN–(O–C(O)Gly-NHC(O))succinyl-Ala-Pro-Ala-AMC (R^2 analogue), for which the cellotetraose structure represents the adjoining cellulose chain of the cotton cellulose nanocrystal.

PAMAM-dendrimer-grafted cellulose nanocrystals (CNC-PAMAM) are prepared by a simple carbodiimide-mediated amidation process. CNC-PAMAM shows strong blue fluorescent emission at three pH values (i.e. pH 3.0, 6.5, and 11.0) (Scheme 5). Phase separation occurs at pH 6.5, and the emission is brighter at pH 3.0 than at pH 11.0; this is indicative of the formation of larger aggregates, which thus affects the fluorescence behavior. Therefore, CNC-PAMAM may have potential applications in the fields of pH-responsive separation, optical imaging, antimicrobials, nanotemplates, and biomedicine owing to its excellent pH-responsive properties, encapsulation capability, and fluorescent emission. In addition, the fluorescence intensity of CNC-PAMAM materials may also be used to determine aggregation levels quickly.

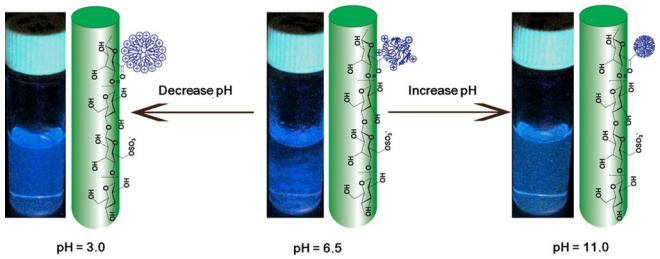

Scheme 5. Schematic representation for the synthesis of CNC-PAMAM. Blue sphere represents one PAMAM dendrimer. Reproduced from Ref. [42] with permission of Elsevier.

4. Conclusions

This Review covered the past decade of research into the use of cellulose as a support for fluorescence sensing. With this Review, we provided a summary of several types of cellulose matrices and various analytes and also discussed the potential applications of these fluorescence-based sensors. We hope that this Review will inspire further research into cellulose-based fluorescence sensors for biologically and medically important species and increase the understanding of the underlying chemistry that is often finely balanced and controlled by the measurement conditions and additional ligands that often control reactivity and influence sensor performance.

Over the next decade, we believe that sensor systems based on cellulose will become increasingly important as people strive to use more environmentally friendly materials. Furthermore, given the diversity of sensors presented within this Review, we anticipate that many other groups will be inspired to explore the numerous benefits provided by cellulose support materials.

Acknowledgements

The authors are grateful for financial support from the National Natural Science Foundation of China (Grant #: 51379077 and Grant #: 21607044). This work was also supported by the Fundamental Research Funds for the Central Universities (2016MS108) and Natural Science Foundation of Hebei Province (B2017502069).

Conflict of Interest

The authors declare no conflict of interest.

Keywords: cellulose · fluorescence · membranes · nanostructures · sensors

[1] a) J. V. Edwards, N. Prevost, K. Sethumadhavan, A. Ullah, B. Condon, *Cellulose* **2013**, *20*, 1223–1235; b) F. Zapata, A. Caballero, P. Molina, A. Tarraga, *Sensors* **2010**, *10*, 11311–11321; c) M. Li, X. Wu, Y. Wang, Y. Li, W. Zhu, T. D. James, *Chem. Commun.* **2014**, *50*, 1751–1753; d) M. Li, H. Ge, R. L. Arrowsmith, V. Mirabello, S. W. Botchway, W. Zhu, S. I. Pascu, T. D. James, *Chem. Commun.* **2014**, *50*, 11806–11809; e) M. Li, G. E. M. Lewis, T. D. James, Y. T. Long, B. Kasprzyk-Hordern, J. M. Mitchels, F. Marken, *ChemElectroChem* **2015**, *1*, 1640–1646; f) J. Yang, M. Li, L. Kang, W. Zhu, *Sci. China Chem.* **2017**, *60*, 607–613.

[2] M. C. Alcudia-León, R. Lucena, A. Soledad Cárdenas, M. Valcárcel, *Anal. Chem.* **2008**, *80*, 1146–1151.

[3] a) E. Eftekhari, W. Wang, X. Li, A. Nikhil, Z. Wu, R. Klein, I. S. Cole, Q. Li, *Sens. Actuators B* **2017**, *240*, 204–211; b) K. B. Pfeifer, K. E. Achyuthan, M. Allen, M. L. Denton, M. P. Siegal, R. P. Manginell, *J. Radiat. Res.* **2017**, *25*, 1–10.

[4] Y. Tao, P. Navaretti, R. Hauert, U. Grob, M. Poggio, C. L. Degen, *Nanotechnology* **2015**, *26*, 465501.

[5] A. Farinha, M. Calvete, F. Paz, *Sens. Actuators B* **2014**, *201*, 387–394.

[6] a) Y. You, H. Zhang, Y. Liu, B. Lei, *RSC Adv.* **2016**, *6*, 90126–90131; b) Y. Xu, B. Lou, Z. Lv, Z. Zhou, L. Zhang, E. Wang, *Anal. Chim. Acta* **2013**, *763*, 20–27; c) J. J. Poole, J. J. Grandy, G. A. Gomezrios, E. Gionfriddo, J. Pawliszyn, *Anal. Chem.* **2016**, *88*, 6859–6866.

[7] a) M. Y. Abdelaal, T. R. Sobahi, R. M. El-Shishtawy, *C. R. Chim.* **2014**, *17*, 557–562; b) B. Bag, A. Pal, *Org. Biomol. Chem.* **2011**, *9*, 4467–4480; c) M. Li, Z. Guo, W. Zhu, F. Marken, T. D. James, *Chem. Commun.* **2015**, *51*, 1293–1296.

[8] a) X. Wang, Y. Guo, D. Li, H. Chen, R. C. Sun, *Chem. Commun.* **2012**, *48*, 5569; b) Y. Tan, J. Yu, J. Gao, Y. Cui, Z. Wang, Y. Yang, G. Qian, *RSC Adv.* **2013**, *3*, 4872–4875; c) E. Sharpe, T. Frasco, D. Andreescu, S. Andreescu, *Analyst* **2013**, *138*, 249–262.

[9] J. L. Morgan, J. Strumillo, J. Zimmer, *Nature* **2013**, *493*, 181–186.

[10] a) J. R. G. Navarro, G. Conzatti, Y. Yang, A. B. Fall, R. Mathew, M. Eden, L. Bergström, *Biomacromolecules* **2015**, *16*, 1293 – 1300; b) I. A. Gilca, V. I. Popa, C. Crestini, *Ultrason. Sonochem.* **2015**, *23*, 369 – 375.
[11] a) M. L. Hassan, C. M. Moorefield, H. S. Elbatal, G. R. Newkome, D. A. Modarelli, N. C. Romano, *Mater. Sci. Eng. B* **2012**, *177*, 350 – 358; b) J. Tang, J. Sisler, N. Grishkewich, K. C. Tam, *J. Colloid Interface Sci.* **2017**, *494*, 397 – 409; c) K. Ishihara, W. Chen, Y. Liu, Y. Tsukamoto, Y. Inoue, *Sci. Technol. Adv. Mater.* **2016**, *17*, 300 – 312.
[12] a) M. Elsakhawy, S. Kamel, A. Salama, H. A. Sarhan, *J. Drug Delivery* **2014**, *2014*, 1 – 6; b) Y. Wang, H. Song, L. Peng, Q. Zhang, S. Yao, *Biotechnol. Biotec. Eq.* **2014**, *28*, 981 – 988.
[13] a) S. Rajesh, K. H. Shobana, S. Anitharaj, D. R. Mohan, *Ind. Eng. Chem. Res.* **2011**, *50*, 5550 – 5564; b) N. Peng, Y. Wang, Q. Ye, L. Liang, Y. An, Q. Li, C. Chang, *Carbohydr. Polym.* **2016**, *137*, 59 – 64; c) Y. Li, H. Xiao, M. Chen, Z. Song, Y. Zhao, *J. Mater. Sci.* **2014**, *49*, 6696 – 6704.
[14] a) E. Feese, H. Sadeghifar, H. S. Gracz, D. S. Argyropoulos, R. A. Ghiladi, *Biomacromolecules* **2011**, *12*, 3528 – 3539; b) F. Wang, Y. Pan, P. Cai, T. Guo, H. Xiao, *Bioresour. Technol.* **2017**, *241*, 482 – 490.
[15] E. L. Lindh, M. Bergenstråhle-Wohlert, C. Terenzi, L. Salmén, I. Furó, *Carbohydr. Res.* **2016**, *434*, 136.
[16] a) N. Lavoine, I. Desloges, A. Dufresne, J. Bras, *Carbohydr. Polym.* **2012**, *90*, 735 – 764; b) K. Missoum, M. N. Belgacem, J. Bras, *Materials* **2013**, *6*, 1745 – 1766.
[17] Y. Yang, X. Fan, Y. Long, K. Su, D. Zou, N. Li, J. Zhou, K. Li, F. Liu, *J. Mater. Chem.* **2009**, *19*, 7290 – 7295.
[18] M. Z. Ongun, K. Ertekin, M. Gocmenturk, Y. Ergun, A. Suslu, *Spectrochim. Acta Part A* **2012**, *90*, 177 – 185.
[19] M. Min, X. Wang, Y. Chen, L. Wang, H. Huang, J. Shi, *Sens. Actuators B* **2013**, *188*, 360 – 366.
[20] Q. Niu, K. Gao, W. Wu, *Carbohydr. Polym.* **2014**, *110*, 47 – 52.
[21] S. Kacmaz, K. Ertekin, D. Mercan, O. Oter, E. Cetinkaya, E. Celik, *Spectrochim. Acta Part A* **2015**, *135*, 551 – 559.
[22] S. Raj, D. R. Shankaran, *Sens. Actuators B* **2016**, *226*, 318 – 325.
[23] X. Zhang, J.G. Huang, *Chem. Commun.* **2010**, *46*, 6042 – 6044.
[24] L. Q. Xu, K. G. Neoh, E. T. Kang, G. D. Fu, *J. Mater. Chem. A* **2013**, *1*, 2526 – 2532.
[25] X. Liu, C. Zong, L. Lu, *Analyst* **2012**, *137*, 2406 – 2414.
[26] G. H. Chen, W. Y. Chen, Y. C. Yen, C. W. Wang, H. T. Chang, C. F. Chen, *Anal. Chem.* **2014**, *86*, 6843 – 6849.
[27] C. Núñez, M. Diniz, A. A. D. Santos, J. L. Capelo, C. Lodeiro, *Dyes Pigm.* **2014**, *101*, 156 – 163.
[28] P. Srivastava, S. S. Razi, R. Ali, R. C. Gupta, S. S. Yadav, G. Narayan, A. Misra, *Anal. Chem.* **2014**, *86*, 8693 – 8699.
[29] J. Rull-Barrull, M. d'Halluin, E. Le Grognec, F.-X. Felpin, *Chem. Commun.* **2016**, *52*, 2525 – 2528.
[30] Y. Bian, B. He, J. Li, *Cellulose* **2016**, *23*, 2363 – 2373.
[31] C. Díez-Gil, R. Martínez, I. Ratera, A. Tárraga, P. Molina, J. Veciana, *J. Mater. Chem.* **2008**, *18*, 1997 – 2002.
[32] D. D. Hong, J. I. Rhee, *Talanta* **2015**, *134*, 333 – 339.
[33] B. B. Campos, L. Gelde, M. Algarra, E. D. S. Jc, M. I. Vázquez, J. Benavente, *Carbohydr. Polym.* **2016**, *151*, 939 – 946.
[34] B. W. Davis, N. Niamnont, C. D. Hare, M. Sukwattanasinitt, C. Quan, *ACS Appl. Mater. Interfaces* **2010**, *2*, 1798 – 1803.
[35] J. Isaad, A. E. Achari, *Tetrahedron* **2011**, *67*, 4939 – 4947.
[36] K. Sibel, E. Kadriye, G. Mustafa, S. Aslihan, E. Yavuz, C. Erdal, *React. Funct. Polym.* **2013**, *73*, 674 – 682.
[37] T. Ikai, D. Suzuki, Y. Kojima, C. Yun, K. Maeda, S. Kanoh, *Polym. Chem.* **2016**, *7*, 4793 – 4801.
[38] F. Xiong, Y. Han, G. Li, T. Qin, S. Wang, F. Chu, *Ind. Crop Prod.* **2016**, *83*, 663 – 669.
[39] G. Yang, X. Wan, Y. Su, X. Zeng, J. Tang, *J. Mater. Chem. A* **2016**, *4*, 12841 – 12849.
[40] Y. Qiang, X. Pan, *J. Appl. Polym. Sci.* **2010**, *117*, 3639 – 3644.
[41] J. V. Edwards, N. T. Prevost, A. D. French, M. Concha, B. D. Condon, *Carbohydr. Polym.* **2015**, *116*, 278 – 285.
[42] L. Chen, W. Cao, N. Grishkewich, R. M. Berry, K. C. Tam, *J. Colloid Interface Sci.* **2015**, *450*, 101 – 108.

Received: July 16, 2017
Version of record online September 18, 2017

